# Cocurrent Flow of Gas-Particulate Mixtures Through Helical Tubular Coils: Particle Velocity Measurement and Prediction

Particle velocities are measured for the cocurrent flow of air and coal particles through helical coils. The ratio of average particle velocity to gas velocity, $V_g$, is nearly independent of $V_g$ at 0.25 ± 0.1. This ratio would be above 0.95 for similar flow conditions in straight, horizontal tubes. The particle velocities also depend slightly on other variables, decreasing with larger particles, larger solids feed rate, and smaller helix diameters. Visual observations reveal that the particles slide along the outer periphery of the coil, in a fashion similar to the sliding action at saltation conditions in horizontal flow. A model that permits prediction of particle velocity in helical geometries is proposed; this model is based on the modification of existing saltation velocity correlations by substituting centripetal acceleration for gravitational acceleration. Approximate agreement between experiment and prediction is obtained.

**Ming-tsai Shu, J. A. Hamshar, and C. B. Weinberger**
Department of Chemical Engineering
Drexel University
Philadelphia, PA 19104

## SCOPE

Velocities of coal particles during cocurrent air flow downward through vertical helical coils are presented as a function of air velocity, particle diameter and density, loading ratio, and helix diameter. The particles are lignite and coal char and range in size from 46 to 350 $\mu$m. Gas velocities range from 7 to 23 m/s and loading ratios from 0.2 to 3.0. Two helix diameters, 98 and 187 mm, are used. Entrapment measurements are used to determine particle velocity.

Another objective includes the development of means to predict particle velocities in helical configurations. This work assumes relevance in gas-solids reactors and transport systems of similar geometry.

## CONCLUSIONS AND SIGNIFICANCE

Gas velocity is the dominant independent variable controlling particle velocity, as the average ratio of particle to gas velocity is about 0.25 ± 0.1. In contrast, the velocity ratio would be above 0.95 for comparable flow conditions in horizontal pipes. As for the other independent variables, $V_p$ increases slightly with larger helix diameter, smaller particle size, and smaller loading ratio.

In contrast to pneumatic transport in horizontal tubes, the particles here appear to be trapped in a saltation type of flow, regardless of gas velocity. Accordingly, a previously existing saltation velocity correlation (Zenz, 1964) was modified by substituting centripetal acceleration for gravitational acceleration. This yields a prediction of particle velocity in helical flow. The prediction scheme appears quite successful, as agreement with experiment was within 25% in all cases.

## Introduction

When particulates are being transported in conduits by a gas stream, there frequently arises the need to estimate the average velocity of the particulates. In reactors one may want to know the particle residence time and, in situations involving heat or mass transfer, one may need to know the slip velocity, or the particle velocity relative to that of the surrounding gas.

There exist several methods and correlations for estimating such particle velocities for vertical or horizontal tubes: Jones et al. (1966), Hinkle (1953), Wen (1971), Ikemori and Munakata (1974), Yang (1973), Yang et al. (1973); however, predictive methods do not exist currently for helically coiled pipes. The typical motivation for using a helical configuration is to achieve greater compactness compared to straight-line runs.

The helical motion of a flowing suspension tends to thrust the particles against the outer periphery of the tube, due to the centrifugal forces on the particles. The action can be compared with that of a gas-solids cyclone separator. Because of this additional centrifugal thrust, the actual particle velocities tend to be much lower than would be predicted from correlations applicable to straight horizontal pipes.

The sliding or skimming action of the particles in helical flow is analogous to saltation flow in horizontal tubes. The saltation velocity is defined as that gas velocity required to keep the particles barely skimming along the bottom of a horizontal pipe. At saltation, the gravitational force on the particles is matched by the lifting force generated by the carrier gas. Similarly, in helical flow the centrifugal force is balanced by this same lifting force.

Since these two physical situations are so similar, the question then arises whether existing correlations for saltation velocity in horizontal flow (Zenz, 1964) can be modified, a priori, to yield predictions for particle velocity in helical flow. The results reported here show that such a predictive scheme is indeed successful. The approach is similar to that used by Kalen and Zenz (1974) in their analysis of cyclone design.

The experimental objectives of this work are to determine the dependence of particle velocity on gas velocity, particle type and diameter, mass flow rate of solids, and helix diameter. The particle types are both coal: a North Dakota lignite, and a coal char (solid product from pilot hydrogenation runs).

## Experimental

A sketch of the apparatus is given in Figure 1. Particle velocities were determined using an entrapment technique with quick-closing valves. The carrier gas, dry air, was fed from a cylinder through a rotameter; the particles were metered from a slightly pressurized hopper using a circumferentially grooved disk driven by a variable-speed motor. After passing through a straight-through, solenoid-actuated valve, the gas-solid suspension passed through the helical coil. The coils, made of glass to permit visual observation of the flowing suspension, were 6.40 m long, with a 7.14 mm I.D. and helix diameters (center-to-center) of either 98.4 or 187 mm. The center-to-center vertical spacing between coils was relatively low, 14 mm. Before existing, the suspension passed through a final solenoid valve.

The gas velocities ranged from 7 to 23 m/s. Gas velocities were limited on the low side to those velocities at which dune formation or tube blockage occurred. The pressure drop through the system was relatively small, on the order of 10 kPa (0.1 atm) or less. The mass flow rate of the particles ranged from 211 to 430 mg/s, equivalent to loading ratios (mass flow rate of solids to air) ranging from 0.187 to 2.90. Size characteristics of the particles are given in Table 1; particle diameters of the lignite (130 to 350 $\mu$m) were slightly greater than those of the coal char (50 to 160 $\mu$m). The lignite was also more dense, 1,490 vs. 720 kg/m$^3$. Microscopic examination of the particles showed the shape of lignite particles to be increasingly irregular and nonspherical with increasing particle diameter; the coal char particles were much more spherical in appearance. Based on free-fall velocity measurements (Shu, 1978), the surface shape factor, $X$, was estimated from the difference between the measured velocity and that expected for spherical particles. $X$ is the

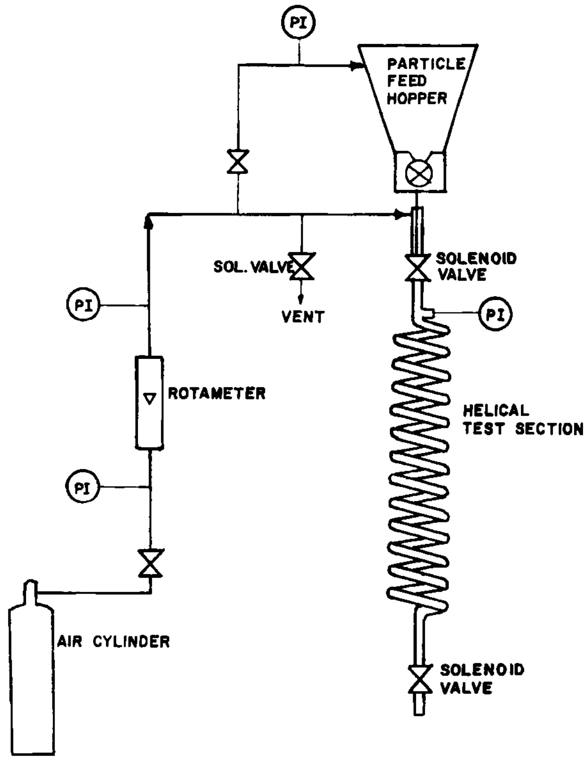


**Figure 1. Diagram of apparatus.**

**Table 1. Particle Size Distribution**

| Sieve Mesh | $d_p$ (log mean) $\mu$m | Mass Fraction wt. % |
|---|---|---|
| | Lignite | |
| 40–50 | 354 | 25.1 |
| 50–60 | 272 | 21.9 |
| 60–70 | 228 | 22.6 |
| 70–100 | 177 | 18.0 |
| 100–140 | 126 | 12.4 |
| | Coal Char | |
| 80–100 | 163 | 8.1 |
| 100–140 | 126 | 28.5 |
| 140–200 | 89 | 30.4 |
| 200–up | 46 | 33.0 |

ratio of surface areas (sphere/particle) for equal volume. For the coal char particles, $X$ was 1.0; for lignite, $X$ ranged from 0.67 for the 354 $\mu m$ particles to 0.96 for the 89 $\mu m$ particles.

Prior to each test, the mass flow rate of the particles was determined by weighing a timed sample of the solids issuing from the coil. This was found to be more accurate (within ±4% by reproducibility tests) than the use of calibrations of solids rate vs. disk feeder rotational speed. After allowing sufficient time to pass to reach steady conditions (between 10 and 50 particle residence times), the solenoid valves were simultaneously actuated, thereby entrapping the solid particles in the test section. A third solenoid valve permitted venting of the incoming air upstream of the test section. The trapped particles were recovered by opening the lower solenoid valve and gently puffing air into the glass coil to move the particles into a waiting receptacle; the particles were then weighed. Reproducibility tests indicated this measurement to be precise within 5% (including sieving loss). These same reproducibility tests did not show any changes with time of particle size distribution along the tube. By comparing the total mass of particles captured, $m\bar{d}_p)$, to the mass flow rate of the solids, $\dot{M}(\bar{d}_p)$, the overall average particle velocity, $V_p(\bar{d}_p)$ could be calculated,

$$V_p(\bar{d}_p) = \frac{\dot{M}(\bar{d}_p)}{m(\bar{d}_p)} L \tag{1}$$

where $L$ is the length of the helical coil. Moreover, the dependence of particle velocity on particle diameter could be determined from comparative sieve analysis of the trapped particles and of the feed material.

$$V_p(d_p) = \frac{\dot{M}(d_p)}{m(d_p)} L \tag{2}$$

where $m(d_p)$ is the mass trapped between two given diameters (that is, between two sieve sizes), and $\dot{M}(d_p)$ is the corresponding feed rate of that particle size range.

Although particle acceleration lengths can be significant in tests such as these, calculations show that the particles should be nearly fully accelerated within 20 mm of the coil entrance, assuming a zero initial velocity. Further, particle speeds were lower in the coil than in the vertical section just upstream of the coil, so that even this estimated distance is too long.

Electrostatic forces can also create problems in tests such as these. Some particles were seen to adhere to the inside wall of the glass coil, and presumably electrostatic forces were responsible. However, the amount adhering was negligible so long as gas velocities remained above 5 m/s. Furthermore, at low gas velocities, it could be observed that only the fines, $<70$ $\mu m$, were adhering and these constituted a small fraction of the entire particle size distribution. Accordingly, we do not believe that electrostatic effects were significant in our tests.

In our experiments, $V_p(\bar{d}_p)$, the overall average particle velocity is about 1–2% less than the overall mass-average velocity. The latter is computed by applying suitable mass fraction weighting functions to the mass-average velocities of Eq. 2. Because $m(d_p)$ is much smaller than $m(\bar{d}_p)$,$V_p(\bar{d}_p)$ is known with greater precision than is $V_p(d_p)$. Accordingly where average velocities are reported, these are $V_p(\bar{d}_p)$.

## Results and Discussion

The principal independent variables, in addition to type of particle, are gas velocity, $V_g$; particle diameter, $d_p$; mass flow rate, $\dot{M}(\bar{d}_p)$; and helix diameter, $D_h$. Since the particle velocity, $V_p$, was found to be nearly proportional to $V_g$, the results are presented in terms of the velocity ratio, $V_p/V_g = \phi$, as a function of the several variables.

For the lignite particles, the dependence of this velocity ratio, $\phi$, on $V_g$ with solids feed rate as a parameter is shown in Figure 2. Perhaps the first notable feature of this plot is the approximate constancy of $\phi$ around 0.2 over a threefold range of $V_g$. This finding is very similar to that of Rizk (1976), who notes the constancy of $\phi$ with varying gas velocity in horizontal tubes. In straight horizontal tubes, however, typical $\phi$ values are above

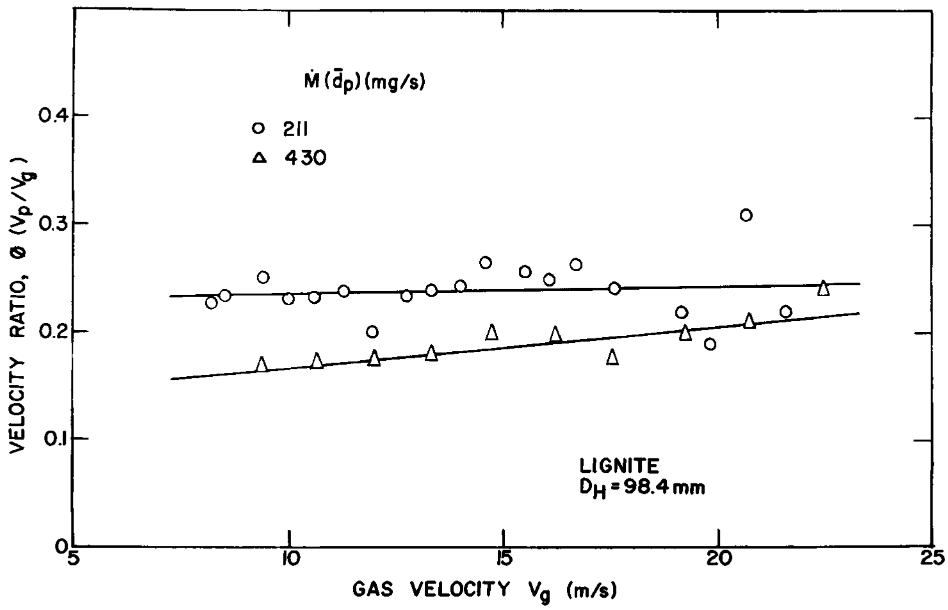


**Figure 2. Effect of solids feed rate and gas velocity on velocity ratio—lignite.**

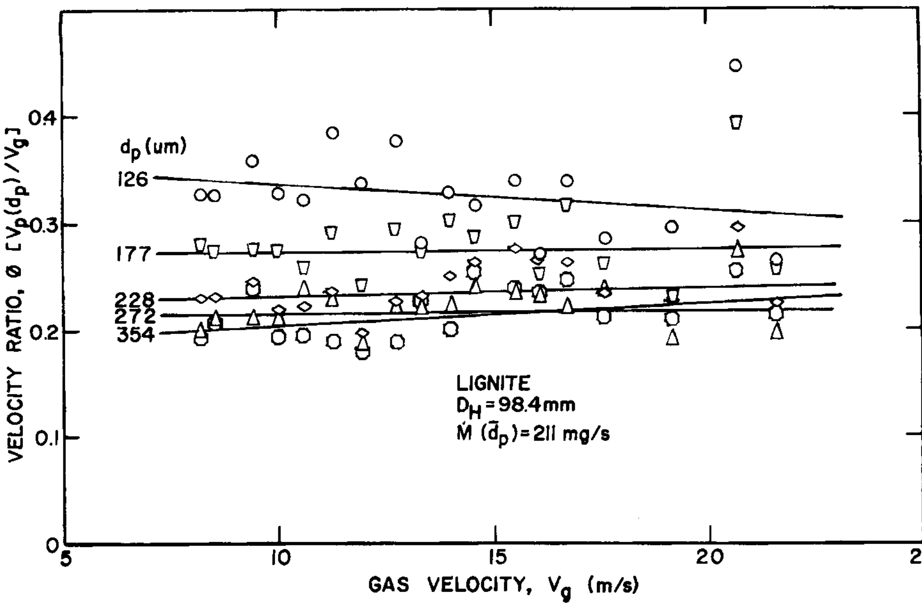


**Figure 3. Effect of particle diameter and gas velocity on velocity ratio—lignite.**

0.95 for particles in this size range. The second notable feature of the plot is the slight decrease in $\phi$ with increased solids feeding rate. Apparently, particle-particle interaction increases at higher feed rates and this leads to increased momentum transfer to the wall and lower average particle velocities. Incidentally, separate tests with vertical downflow in straight tubes (Shu, 1978) do not reveal such a dependence at equivalent flow rates. Of course, in the vertical flow tests the flow appeared homogeneous, whereas in helical flow, a separated or stratified flow could be observed, with the solids concentrated against the outer periphery of the helical coil. Although difficult to estimate, this region of concentrated suspension appeared to occupy roughly one-fifth of the tubular crosssection. The word concentrated is used advisedly, since the overall gas volume fraction in all cases exceeds 0.99. For this volume fraction the particle velocity predicted from correlations for straight tubes is only 4% less than that at infinite dilution.

As for particle diameter, in Figure 3 $\phi$ increases with decreasing $d_p$. This is consistent with the finding of Rizk (1976) with straight horizontal tubes. In addition, this trend can be explained in terms of surface-to-volume ratio. The smaller particles, with a higher ratio, should encounter a relatively higher lifting force, which varies with surface area, compared to the centrifugal force, which varies with particle volume.

For coal char, the results show much the same trends as with lignite. In Figure 4, $\phi$ is about 0.25, approximately independent of $V_g$, and decreases slightly with increasing solids feed rate. Comparing Figures 2 and 4, we note that the velocity ratio $\phi$

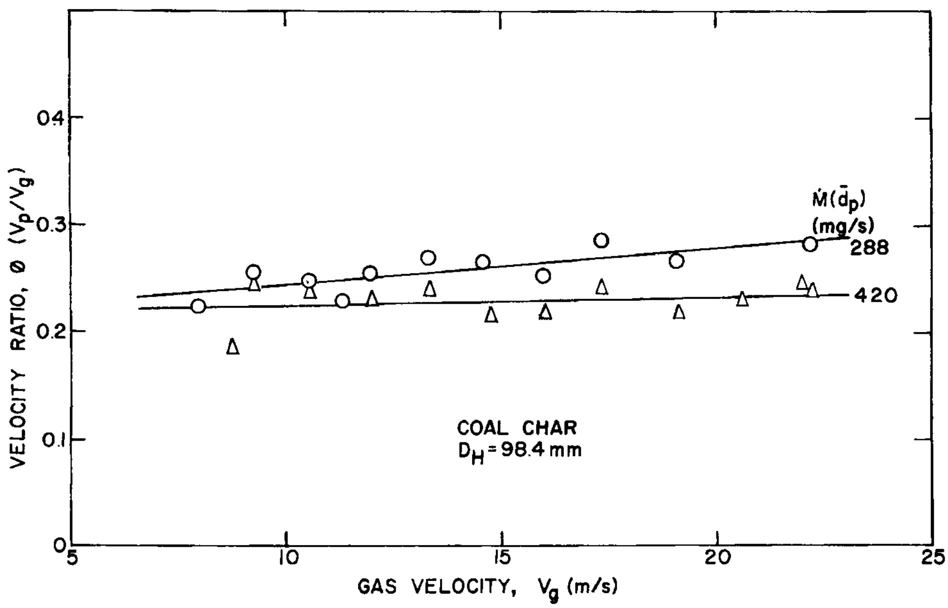


**Figure 4. Effect of solids feed rate and gas velocity on velocity ratio—coal char and small helix diameter.**

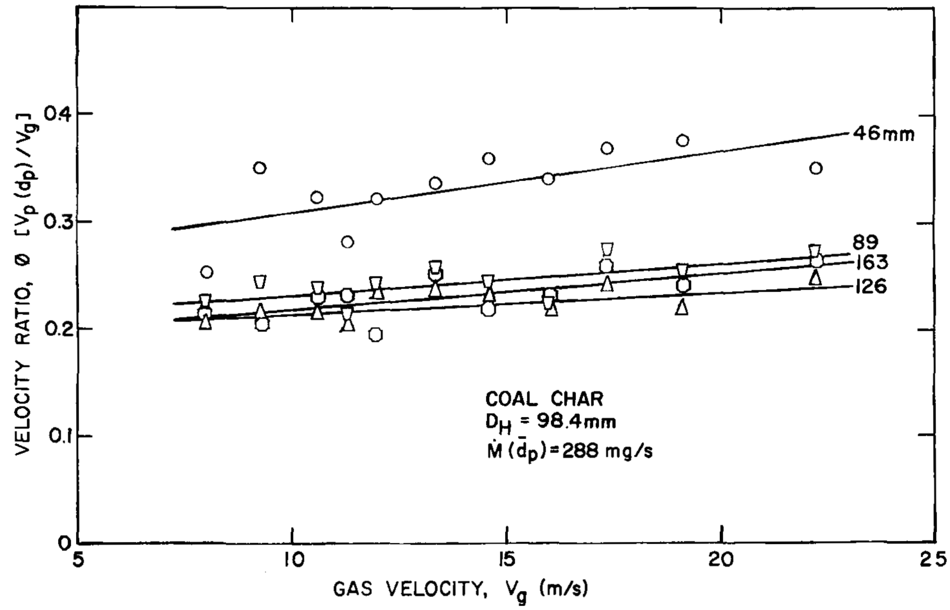


**Figure 5. Effect of particle diameter and gas velocity on velocity ratio—coal char.**

tends to be only slightly higher for the coal char, despite the nearly twofold smaller average $d_p$ and $\rho_p$ for the char. This small change in $\phi$ may be attributable to the greater asphericity and consequently greater specific surface area of the lignite particles.

In Figure 5, the smaller particles again can be seen to possess higher velocity ratios. In the 90 to 160 $\mu$m range, the effect appears to be slight, however.

The effect of helix diameter on particle velocity was investigated using the coal char material. One might expect that larger helix diameters would lead to lower centrifugal forces and thus higher particle velocities; this, indeed, proves to be the case, as shown in Figures 6a and 6b. The effect is slight, however, with $\phi$ increasing from about 0.25 to about 0.30 for a twofold increase in helix diameter. This slight change is not totally unexpected, since the centripetal acceleration, $2(V_p)^2/D_h$, decreases by less than a factor of two.

Summarizing the experimental findings: we observe that over the ranges of variables studied, $\phi$ varies from 0.16 to 0.39, decreasing with increasing solids flow rate and particle diameter and increasing with increasing helix diameter. Except for the effect of helix diameter, these trends are similar to those observed with horizontal flow.

## Prediction of $V_p$

In the current experiments, the centrifugal force on the particles was 5 to 50 times the gravitational force. This provides

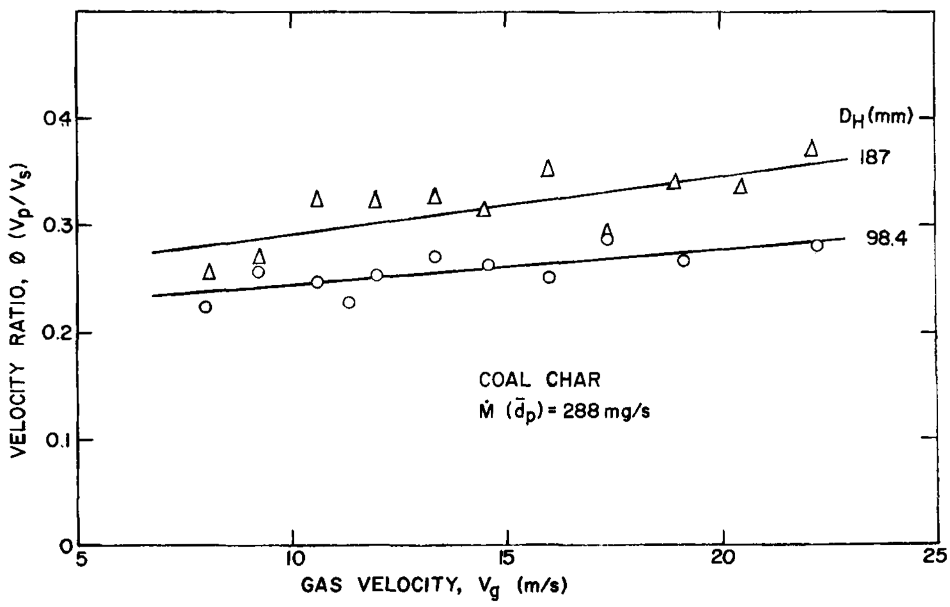


**Figure 6a. Effect of helix diameter on velocity ratio—coal char: low solids feed rate.**

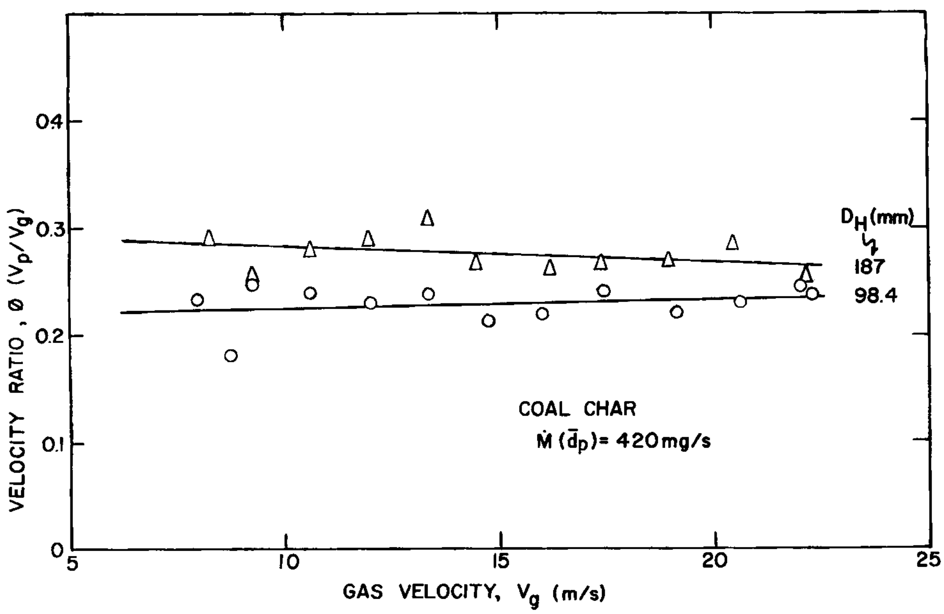


**Figure 6b. Effect of helix diameter on velocity ratio—coal char: high solids feed rate.**

partial justification for the substitution of centripetal acceleration for $g$ in a given saltation velocity correlation to permit prediction of particle velocities.

The particular correlation chosen is that of Zenz (1964). Jones and Leung (1978) review various saltation correlations and note that the Zenz correlation is well-used and widely accepted. Furthermore, it accounts quantitatively for wide particle size distribution, something the other correlations do not. Jones and Leung do show that the Thomas (1962) correlation is more accurate; however, the Thomas correlation does not contain a gravity term, through a Froude number for example, and therefore cannot be modified according to the scheme described here. Other correlations, including those of Rizk (1976), Doig and Roper (1963), Mewing (1976), and Matsumoto et al. (1974), were also tried by this modification scheme. Compared to the modified Zenz correlation predictions, agreement between prediction and experiment was poor. These other correlations predicted particle velocities two to three times too high.

Zenz (1964) describes an empirical correlation for predicting the saltation velocity for single particles, as well as separate correlations permitting prediction of the effects of solids flow rate and particle size distribution. The saltation velocity correlation is basically a correlation of the lifting force required to balance the gravitational force. These correlations, presented in the form of dimensionless groups, are based upon an approximate theoretical analysis of the flow. For the saltation velocity correlation, the group

$$\left[\frac{Re_p}{C_D}\right]^{1/3} = \left[\frac{3V_{so}^3\rho_g^2}{4g\mu_g(\rho_p-\rho_g)}\right]^{1/3} \tag{3}$$

is plotted vs. the group

$$[C_D Re_p^2]^{1/3} = \left[\frac{4d_p^3 g(\rho_p - \rho_g)\rho_g}{3\mu_g^2}\right]^{1/3} \tag{4}$$

where $Re_p$ is a particle Reynolds number and $C_D$ is the particle lifting coefficient, and the remaining variables have the usual definition. $V_{so}$ is the superficial gas velocity at the point of saltation of a single particle or, simply, the saltation velocity. In the Zenz correlation, the first group is a relatively weak function of the second and additional parameters include tube diameter and particle sphericity. In order to modify these correlations for helical flow, the gravity term $g$ in the correlations is replaced simply with $V_p^2\max/R_h$, the corresponding centripetal acceleration term, and the velocity variable in $Re_p$ and $C_D$ is changed from $V_{so}$ to the slip velocity, $V_{so} - V_p$ max. The single-particle saltation-velocity correlation is thereby changed to a plot of

$$\text{Ordinate} = \left[\frac{3(V_{so} - V_p\max)^3\rho_g^2 R_h}{4V_p^2\mu_g(\rho_p - \rho_g)}\right]^{1/3} \tag{5}$$

vs.

$$\text{Abscissa} = \left[\frac{4d_p^3 V_p\max(\rho_p - \rho_g)\rho_g}{3R_h\mu_g^2}\right]^{1/3} \tag{6}$$

where $R_h$ is the helix radius. $V_p$max is the single-particle velocity at which the centrifugal and lifting forces are balanced. Otherwise, except for a tube diameter correction, the same correlation plot is used.

In horizontal pipes, an increase in the gas velocity beyond the saltation velocity will tend to lift all the particles, forming a nearly homogeneous flowing mixture. In contrast, in the helical system an increase in gas velocity does not move beyond saltation conditions. Rather, the gas velocity is always at the saltation velocity, regardless of its magnitude and the lifting force is balanced by the centrifugal force on the particles. As a result, for a given gas velocity, the particle velocity "self-adjusts" to yield balancing centrifugal and lifting forces.

At sufficiently large helix diameter, the system will undergo a transition from saltation to well-dispersed flow. That is, as curvature is reduced centrifugal forces become less important and straight-tube correlations become appropriate. One method to estimate when this situation occurs is to estimate particle velocity from correlations for horizontal, well-dispersed flow. If this velocity is less than the particle velocity estimated for saltation flow in a helix, the centrifugal force should be sufficiently low that well-dispersed conditions result. The particle velocity predicted from horizontal-flow correlations could then be expected to be only slightly greater than the actual velocity. However, since all of our experiments appeared to correspond to a saltation flow, we were not able to test this procedure.

Using the modified Zenz correlations, the first quantity calculated is the single-particle velocity, $V_p\max$. $V_p\max$ is termed a maximum velocity because higher particle velocities would correspond to a situation in which the centrifugal force exceeds the lifting force.

Since the tube diameters used for the Zenz correlation are four to nine times those of the present work, we had to account for the effect of $D_t$. Previous workers report that the saltation velocity, $V_{so}$, is proportional to $D_t$ raised to a power that depends upon particle diameter. An exponent of 0.2, reported by Cairns et al. (1960) for particles in our size range, was used.

For horizontal tubes, a finite solids feed rate tends to increase the saltation velocity beyond $V_{so}$ (Zenz, 1964). We assume here an identical dependence for helical coils. Zenz presents a plot (his Figure 11) of $V_s/V_{so}$ as a function of $\dot{M}/A\rho_p$ with the quantity $S_\Delta$ as a parameter. $V_s/V_{so}$ is the ratio of saltation velocity under loading conditions to that of a single particle and $\dot{M}/A\rho_p$ is the superficial particle mass velocity. $S_\Delta$ is a particle size and size distribution coefficient which can be determined from single-particle horizontal saltation velocity predictions for the various particle sizes. For helical flow the function $V_s/V_{so}$ is replaced by the slip velocity ratio $(V_g - V_p)/(V_{so} - V_p\max)$, where $V_g$ is the corresponding gas velocity for finite $\dot{M}$ and a mixed particle size distribution. The particle diameter associated with $V_p\max$ corresponds to that with the highest saltation velocity in horizontal flow.

Summarizing the specific steps in the particle-velocity prediction scheme, we presume that gas velocity, tube and helix diameter, solids feed rate, and particle size characteristics are specified. First $V_p\max$ is calculated from Figure 3 of Zenz (1964), using the modified coordinate variables, Eqs. 5 and 6, and the tube diameter correction to the ordinate variable. In this calculation, $V$ can initially be estimated as the gas velocity, although it will be corrected in subsequent steps to account for finite solids feed rate and slip. Next, $V_p(\bar{d}_p, V_g)$ is calculated from

$$V_p(\bar{d}_p) = \left[\sum_i \frac{W_i(d_p)}{V_{p_i\max}(d_p)}\right]^{-1} \tag{7}$$

where $W_i(d_p)$ is the mass fraction of particles in the feed within given particle diameters. From Figure 3 of Zenz (using horizontal flow coordinates) and particle size distribution data, the parameter $S_\Delta$ is computed; this parameter, along with Figure 11 of Zenz, is used to estimate the required $V_g$ to yield $V_p(\bar{d}_p)$ at a finite solids feed rate. This $V_g$ is compared to the design gas velocity; if different, the initial guess of a fictitious gas velocity $V_{so}$ is adjusted in the first step. Iteration continues until $V_g$ matches the design gas velocity.

A test of this predictive scheme for the present experimental results is shown in Figure 7. We note that the standard deviation between predicted and experimental velocities is only 7%. Since no new empirical correlations are used in this prediction scheme,

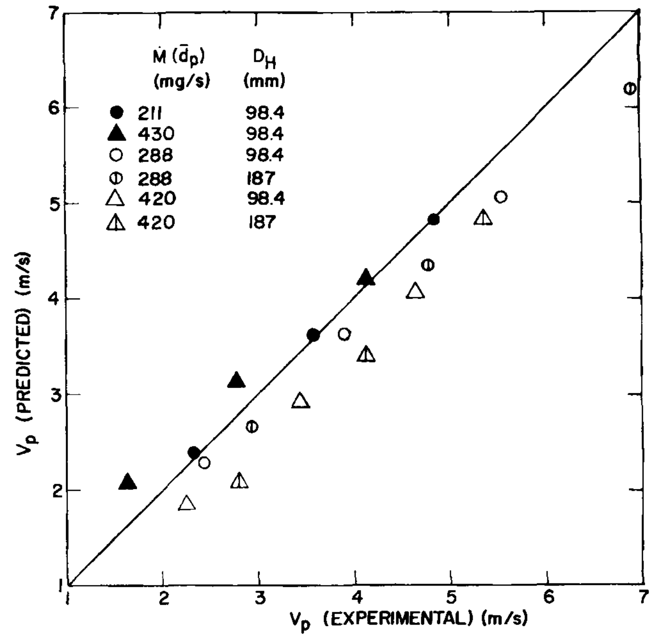


**Figure 7. Test of prediction scheme for particle velocities in helical entrained flow. Filled symbols, lignite; open symbols, coal char.**

this agreement is quite remarkable. There are some consistent discrepancies, however. The predicted values for $V_p(\bar{d}_p)$ are higher than the experimental values for the lignite particles and less for the coal char. Also, there is better agreement between prediction and experiment for the lower solids flow rates, although the direction of the discrepancy differs between lignite and coal char. The question of whether these discrepancies can be attributed to experimental errors or to shortcomings in the prediction method must be answered by further work. Another encouraging aspect of the results is the successful prediction of the effect of helix diameter, $D_h$, for the coal particles; the relative agreement between experimental and predicted velocities remains nearly constant for those tests in which only $D_h$ was changed. This lends additional support to the validity of the prediction scheme.

## Summary

Particle velocities in helical flow of suspensions are significantly lower than the gas velocities. For particles with a $d_p$ of the order of 100 μm and helix diameter of about 100 mm, the ratio of particle velocity to gas velocity is roughly 0.25. This ratio increases with increasing helix diameter and decreasing solids flow rate and decreasing particle diameter.

The particle velocity and its dependence on specific variables can be predicted from the Zenz correlations for saltation velocity in horizontal tubes, once these correlations are modified by using slip velocity for gas velocity and centrifugal force for gravitational force. The standard deviation between predicted and experimental particle velocities is only 7%.

## Notation

$A$ = cross-sectional area of the tube
$C_D$ = lifting coefficient, $4gd_p(\rho_p - \rho_g)/3\rho_g(V_g - V_p)^2$
$D_H$ = helix diameter

$d_p$ = log mean particle diameter between two appropriate sieve sizes
$D_t$ = inside tube diameter
$g$ = gravitational constant
$L$ = length of the helical tube
$\dot{M}(\bar{d}_p)$ or $\dot{M}$ = total solids feeding rate
$\dot{M}(d_p)$ = solids feeding rate of particles with log mean diameter $d_p$
$m(\bar{d}_p)$ = total mass trapped between the two solenoid values
$m(d_p)$ = the trapped mass of particles with log mean diameter $d_p$ trapped between the two solenoid valves
$Re_p$ = particle Reynolds number, $[\rho_g(d_p(V_{so} - V_p))]/\mu_g$
$R_H$ = helix radius
$S_\Delta$ = particle size and size distribution coefficient defined in Zenz's (1964) correlation
$V_g$ = superficial gas velocity
$V_p$ = particle velocity
$V_p(d_p)$ = particle velocity of particles with log mean diameter, $d_p$
$V_{p_{max}}$ = maximum attainable particle velocity in helical flow
$V_{so}$ = superficial gas velocity at saltation of a single particle
$V_s$ = superficial gas velocity at saltation of multiple particles
$\mu_g$ = gas viscosity
$\rho_p$ = particle density
$\rho_g$ = gas density
$\phi$ = velocity ratio, $V_p/V_g$

## Literature Cited


Cairns, R. C., K. R. Lawther, and K. S. Turner, "Flow Characteristics of Dilute Small Particle Suspensions," *Brit. Chem. Eng.*, **5**, 849 (1960).
Doig, I. D., and G. H. Roper, *Aust. Chem. Eng.*, **4**, 9 (1963).
Hinkle, B. L., "Acceleration of Particles and Pressure Drops in Horizontal Pneumatic Conveying," Ph.D. Thesis, Georgia Inst. Technology (1953).
Ikemori, K., and H. Munakata, "A New Method of Expressing Pressure Drop in Horizontal Pipe Bend," *Proc. Pneumotransport*, **2**, A3 (1974).
Jones, J. H. et al., "Slip Velocity of Particulate Solids in Vertical Tubes," *AIChE J*, **12**, 1,070 (1966).
Jones, P. J., and L. S. Leung, "A Comparison of Correlations for Saltation Velocity in Horizontal Pneumatic Conveying," *Ind. Eng. Chem. Proc. Des. Dev.* **17**, 571 (1978).
Kalen, B., and F. A. Zenz, "Theoretical-Empirical Approach to Saltation Velocity in Cyclone Design," *AIChE Symp. Ser.* **70**, 388 (1974).
Matsumoto, S., et al., "Minimum Transport Velocity for Horizontal Pneumatic Conveying," *J. Chem. Eng. Japan*, **7**, 425 (1974).
Mewing, S. F., B. E. Thesis, Univ. Queensland, Australia (1976).
Rizk, F. "Pneumatic Conveying at Optimal Operation Conditions and a Solution of Barth's Equation," *Proc. Pneumotransport*, **3**, (1976).
Shu, M-T, "Concurrent Two-Phase Flow of Gas and Coal Particle Mixtures," M.S. Thesis, Drexel Univ., Philadelphia, PA (1978).
Thomas, D. G. "Transport Characteristics of Suspensions," *AIChE J.*, **8**, 373 (1962).
Wen, C. Y., *Bulk Material Handling*, M. C. Hawk, ed., Univ. of Pittsburgh, **1**, 258 (1971).
Yang, W. C., "Estimating the Solid Partical Velocity in Vertical Pneumatic Conveying Lines," *Ind. Eng. Chem. Fund.*, **12**, 349 (1973).
Yang, W. C., D. L. Keairns, and D. H. Archer, "Estimating the Solid Particle Velocity in Horizontal Pneumatic Conveying Lines," *Can. J. Chem. Eng.*, **51**, 779 (1973).
Zenz, F. A., "Conveyability of Materials of Mixed Particle Size," *Ind. Eng. Chem. Fund.*, **3**, 65 (1964).


*Manuscript received Feb. 8, 1982, and revision received Apr. 30, 1985.*